


RESEARCH ARTICLE | MAY 14 2024

On-chip quasi-light storage for long optical delays using Brillouin scattering ^{EP}

Special Collection: [Brillouin Scattering and Optomechanics](#)

Moritz Merklein ; Lachlan Goulden ; Max Kiewiet ; Yang Liu ; Choon Kong Lai ; Duk-Yong Choi ; Stephen J. Madden; Christopher G. Poulton ; Benjamin J. Eggleton 

 Check for updates

APL Photonics 9, 056107 (2024)
<https://doi.org/10.1063/5.0193174>



Articles You May Be Interested In

On-chip stimulated Brillouin scattering via surface acoustic waves

APL Photonics (October 2024)

100 years of Brillouin scattering: Historical and future perspectives

Appl. Phys. Rev. (November 2022)

Brillouin laser spectrometer based on spectral compression

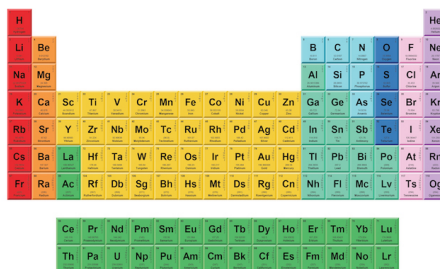
APL Photonics (July 2023)

05 December 2024 16:24:32



THE MATERIALS SCIENCE MANUFACTURER®

Now Invent.™



American Elements
 Opens a World of Possibilities

...Now Invent!

www.americanelements.com

© 2024 American Elements & U.S. Registered Trademark

On-chip quasi-light storage for long optical delays using Brillouin scattering

Cite as: APL Photon. 9, 056107 (2024); doi: 10.1063/5.0193174

Submitted: 21 December 2023 • Accepted: 29 April 2024 •

Published Online: 14 May 2024



View Online



Export Citation



CrossMark

Moritz Merklein,^{1,2,a)}  Lachlan Goulden,^{1,2}  Max Kiewiet,^{1,2}  Yang Liu,^{1,2}  Choon Kong Lai,^{1,2} 
Duk-Yong Choi,³  Stephen J. Madden,³ Christopher G. Poulton,⁴  and Benjamin J. Eggleton^{1,2} 

AFFILIATIONS

¹Institute of Photonics and Optical Science (IPOS), School of Physics, The University of Sydney, Sydney, NSW 2006, Australia

²Univeristy of Sydney Nano Institute (Sydney Nano), The University of Sydney, Sydney, NSW 2006, Australia

³Laser Physics Centre, Research School of Physics, The Australian National University, Canberra, ACT 2601, Australia

⁴School of Mathematical and Physical Sciences, University of Technology Sydney, Sydney, NSW 2007, Australia

Note: This paper is part of the APL Photonics Special Topic on Brillouin Scattering and Optomechanics.

^{a)}Author to whom correspondence should be addressed: moritz.merklein@sydney.edu.au

ABSTRACT

Efficient and extended light storage mechanisms are pivotal in photonics, particularly in optical communications, microwave photonics, and quantum networks, as they offer a direct route to circumvent electrical conversion losses and surmount bandwidth constraints. Stimulated Brillouin Scattering (SBS) is an established method to store optical information by transferring it to the acoustic domain, but current on-chip SBS efforts have limited bandwidth or storage time due to the phonon lifetime of several nanoseconds. An alternate approach known as quasi-light storage (QLS), which involves the creation of delayed replicas of optical data pulses via SBS in conjunction with a frequency comb, has been proposed to lift the storage time constraint; however, its realization has been confined to lengthy optical fibers, constraining integration with on-chip optical elements and form factors. Here, we present an experimental demonstration of QLS on a photonic chip leveraging the large SBS gain of chalcogenide glass, achieving delays of up to 500 ns for 1 ns long signal pulses, surpassing typical Brillouin storage processes' acoustic lifetime by more than an order of magnitude and waveguide transit time by two orders of magnitude. We experimentally and numerically investigate the dynamics of on-chip QLS and reveal that the interplay between the acoustic wave that stores the optical signal and subsequent optical pump pulses leads to a reshaping of the acoustic field. Our demonstrations illustrate the potential for achieving ultra-long storage times of individual pulses by several hundred pulse widths, marking a significant stride toward advancing the field of all-optical storage and delay mechanisms.

© 2024 Author(s). All article content, except where otherwise noted, is licensed under a Creative Commons Attribution-NonCommercial-NoDerivs 4.0 International (CC BY-NC-ND) license (<https://creativecommons.org/licenses/by-nc-nd/4.0/>). <https://doi.org/10.1063/5.0193174>

I. INTRODUCTION

Optical pulse delay methods provide an essential building block for optical signal processing applications such as beam steering in phased array antennas for RADAR and wireless communications,^{1,2} buffering in optical communication links,³ quantum memories,⁴ and tunable optical and microwave photonic filters.^{5,6} There are multiple approaches to all-optical signal delay; these can be broadly categorized into techniques that lengthen the distance light travels,^{7–9} those that slow down the speed of light signals (slow light),^{10–16} and techniques that convert the signal information from light to another—slower wave—which is then recovered at a later

time.^{17,18} Stimulated Brillouin Scattering (SBS) is a third order non-linear optical phenomenon that coherently couples slow-moving acoustic waves with optical waves.^{19,20} SBS involves the interaction between three different waves: the optical pump wave at frequency ω_p , an acoustic wave at the Brillouin frequency Ω_B , and an optical probe or Stokes wave at $\omega_s \approx \omega_p - \Omega_B$, which moves in the opposite direction to the pump.²¹ This three-wave interaction has an extremely narrow linewidth response proportional to the inverse of the acoustic lifetime. SBS has been shown to be a powerful method for implementing different all-optical signal delay methods,²² such as Brillouin-grating based delay lines,^{7,8} slow-light,^{16,23} and light storage,¹⁷ which all operate at room temperature and, in the case of

slow-light and Brillouin light storage, can be implemented on a photonic chip.^{18,22,24,25} However, the fractional delay (a ratio of induced delay over pulse-duration) of Brillouin-based slow-light is essentially limited to values of ~ 1 because the achievable delay is directly proportional to the bandwidth over which the delay can be applied (this effect is also often referred to as the delay-bandwidth product).²⁶ Longer delays can be achieved using Brillouin light storage,^{17,18} in which Brillouin scattering is used to transfer the information carried by the optical data pulses to the much slower acoustic wave packets; fractional delays much larger than one were achieved on a chip-based platform using this method.¹⁸

In Brillouin light storage, the bandwidth of the signal pulses that can be delayed is limited by the Brillouin gain, while the storage time is ultimately limited by the phonon lifetime. Although this can be circumvented by refreshing the data with an additional write pulse,²⁷ Brillouin light storage times are still limited to several tens of nanoseconds. An alternative approach that does not have this inherent limitation is SBS-based quasi-light storage (QLS).^{28,29} In QLS, the optical signal pulse is copied by repeated multiplication with an optical pulse-train, which can be described as a sampling of the signal pulse bandwidth with a frequency comb in the frequency domain. Time delays in the tens of nanoseconds²⁸ and even exceeding 100 ns by narrowing the Brillouin linewidth³⁰ were achieved using QLS. However, the existing demonstrations of QLS have relied on having long lengths (5–20 km, transit time/latency: 25–100 μ s) of optical fiber due to the weak acousto-optic interaction (or low Brillouin gain coefficient) that requires consecutive amplification of the signal pulse over a long traveling distance, in which the SBS interaction can take place.²⁸ However, this need for long interaction lengths impedes the demonstration of QLS in integrated photonic devices.

In this paper, we experimentally demonstrate SBS-based QLS in a waveguide on a photonic chip, in which the strong Brillouin effect in chalcogenide waveguides enables the generation of slow-moving acoustic wave packets by merely a single pump pulse. The acoustic wave is sustained by successive pump pulses, in the meantime generating delayed pulse copies. We achieve 500 ns of delay for a pulse width of ~ 1 ns, greatly exceeding the intrinsic phonon lifetime of ~ 10 –12 ns and the waveguide transit time of 2 ns. We investigate how the delay time depends on the optical signal pulse timing and the pump pulse repetition rate, and examine the retention of the original data pulse shape over successive interactions with the

pump. Our modeling demonstrates that consecutive pulse interactions reshape the acoustic wave, drawing it toward the front facet of the waveguide, in line with our experimental findings. Moreover, our research indicates that sufficient energy imparted during the interaction can sustain and potentially amplify the acoustic pulse by overcoming its intrinsic losses. As the acoustic pulse reaches and resides at the waveguide's front facet, it exhibits endurance over extensive durations, although with observed distortions in the output pulse shape. This comprehensive study sheds light on the intricate dynamics of SBS-based QLS, offering insights into the manipulation and sustainability of acoustic pulses within waveguides, paving the way for prolonged and controlled light storage.

II. BASIC PRINCIPLE

The basic principle of SBS-based QLS is illustrated in Fig. 1, based on the convolution theorem: the multiplication of two signals in the frequency domain is equivalent to a convolution in the time domain.²⁸ Multiplying a signal pulse in the frequency domain with a frequency comb creates multiple copies of the original signal in the time domain, as shown in Fig. 1(a). One of these copies can then be isolated using an optical switch, effectively creating a delayed version of the original signal. This multiplication in the frequency domain is performed by SBS, which creates a narrow (10–100 MHz) gain response that can be used for spectral sampling. The time domain dynamics of the process are shown in Fig. 1(b): a train of pulses centered at the pump frequency ω_p enters the waveguide from the right-hand side (in the following, we refer to the facet of the waveguide from where the pump enters the chip as the “front facet”). A signal pulse, centered at the Stokes frequency ω_s , enters the waveguide from the left. When the first of the pump pulses meets the signal pulse, an acoustic wave is created that “stores” the information (shape, phase, and timing) of the signal pulse. Further pump pulses partially reflect off this acoustic wave, resulting in “copies” of the signal stored in the acoustic wave. This is very similar to the process of writing to and reading from the acoustic wave seen in SBS light storage,^{18,27} with the key difference that here the stored pulses are at the Stokes frequency rather than at the frequency of the pump, and every consecutive pump pulse replenishes the otherwise decaying acoustic wave. In optical fiber, in contrast, the optical signal pulse

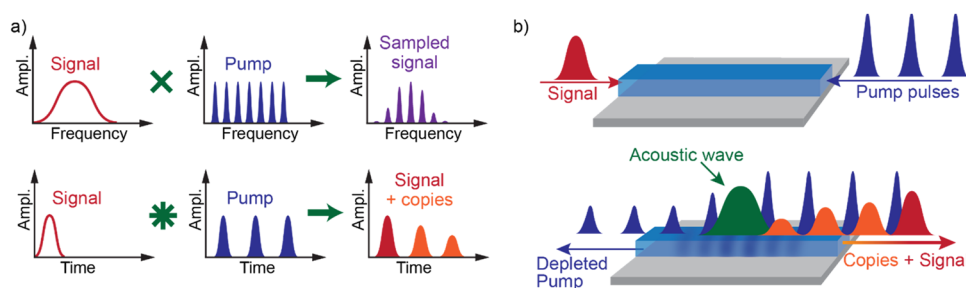


FIG. 1. Principles of QLS. (a) The frequency domain explanation: multiplication of the frequency representations of the pump and signal by SBS is equivalent to the convolution of the time representations. (b) The time domain explanation: the signal (probe) and pump enter the chip from opposite sides. Where they meet in the chip, they create an acoustic wave. Each subsequent pump pulse scatters off the acoustic wave, creating copies of the signal.

interacts with the counter-propagating pulse train at multiple locations along the several kilometers of fiber, creating multiple acoustic waves in the process.

III. EXPERIMENTAL RESULTS

The setup used in the experiments is shown in Fig. 2(a). A 1550 nm laser was split into two arms: the “pump” and “signal” arms. The light in the signal arm was downshifted from the pump frequency by the Brillouin frequency shift Ω_B of the chalcogenide waveguide (7.72 GHz) with an intensity modulator (IM) driven by a radio frequency (RF) signal generator (SG). The lower-frequency sideband was selected using a narrow band filter (NBF). Afterward, a signal pulse was modulated onto the probe via a second IM connected to an arbitrary waveform generator (AWG). The signal was amplified by erbium-doped fiber amplifiers (EDFAs), followed by broadband optical filters (BBFs) (a bandwidth of ~ 2 nm) to reduce excess wide-band amplified spontaneous noise from the EDFAs. On the pump side, an electrical frequency comb was generated using an AWG that drives an IM. The pump was then amplified with an EDFA. The pump and the signal were coupled from opposite sides into the on-chip waveguide. The waveguide was a small-footprint 23-cm-long chalcogenide (As_2S_3) spiral rib waveguide;³¹ a typical chalcogenide chip is shown in Figs. 2(b) and 2(c). The 23 cm-long-spiral waveguides have a cross section of $2.2 \mu\text{m} \times 960 \text{ nm}$ with a 33% etch depth, a varying bend radius from 220 to 180 μm , and a propagation loss of 0.4 dB/cm. The length of the waveguide limits the maximum pulse length to 1–2 ns, as one needs to ensure that the pump and signal pulses are spatially overlapping in the waveguide.

Vertical tapers were used to transition from the chalcogenide waveguide to Germanosilicate waveguides at both ends of the chip; these Germanosilicate waveguides minimize the refractive index mismatch between the chip and optical fiber and reduce the back-reflection as outlined in Ref. 31. Whereas the waveguide is optically multi-moded, we ensure that light is coupled into the quasi-transverse electric (TE) mode by minimizing the overall loss. The

acoustic mode is guided in the waveguide core via total internal reflection due to a contrast in the acoustic impedance.³²

The light was coupled into the chip using ultra-high numerical aperture (UHNA-3) fiber, with index matching fluid between the fiber and chip interface to maximize coupling efficiency and further reduce back-reflection. Circulators were used on both sides of the photonic chip to separate the counter-propagating optical signals. A photodetector (PD, Newport 1544-A 12 GHz) and an oscilloscope (12 GHz analog bandwidth, Keysight Infiniium) were used to measure the original signal pulses and the delayed copies of the signal. An optical NBF before the PD was used to ensure that only the signal pulses and delayed copies were detected. To confirm that only the signal, and not the residual pump, is measured by the PD, an optical spectrum analyzer (OSA) was used to monitor the optical spectrum after the NBF.

A. On-chip QLS and the effects of pump repetition rate

We show the results from the Brillouin-based QLS experiment in Fig. 3. The original signal pulse (black) is strongly amplified by the first pump pulse and is followed by a sequence of copies that have been generated from the stored acoustic wave by the following pump pulses. Figure 3(b) shows a zoomed-in original signal pulse and the first created copy. We studied the dynamics of different pump repetition rates on the decay of the copies (in particular the first one) using five different pulse trains of 21 successive Gaussian pulses with 500 ps full-width at half maximum (FWHM). We varied the pulse train repetition rate from 100, 125, 150, and 175–200 MHz. The peak power of the pump pulses was kept constant at 10.8 W (we note that the pulse peak power rather than average power was kept constant as the peak power determines the dynamics of the nonlinear Brillouin interaction). The signal pulse was a single 1 ns FWHM Gaussian pulse with a peak power of 19.7 W and was kept the same for different pump repetition rates. In Figs. 3(a) and 3(b), it can be seen that the repetition rate has a major effect on the evolution of the amplitudes of the copied signals. While the initial signal pulse

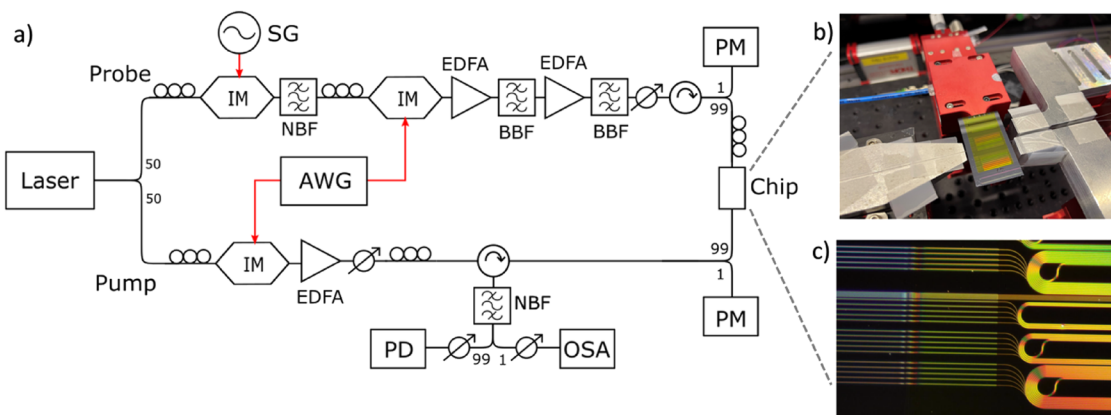


FIG. 2. (a) Experimental setup. SG: Signal Generator, IM: Intensity Modulator, EDFA: Erbium Doped Fiber Amplifier, AWG: Arbitrary Waveform Generator, PD: Photodetector, PM: Power Meter, OSA: Optical Spectrum Analyzer, NBF: Narrowband Filter, and BBF: Broadband Filter. (b) Photo of the chalcogenide chip used in the experiment on the coupling stage. (c) Zoom-in on chalcogenide spiral rib waveguides with different lengths on a photonic chip.

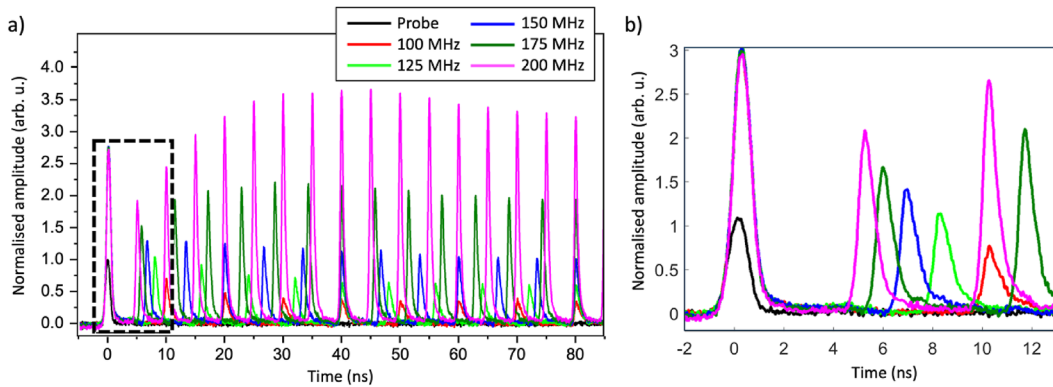


FIG. 3. (a) Demonstration of on-chip Brillouin QLS for different pump repetition rates. The original signal pulse is shown in black. (b) Enlarged plot of the boxed region in (a), showing the first copies for each repetition rate and exhibiting the exponential decay associated with the phonon lifetime.

is amplified by the same amount in each case, the amplitude of the first copy follows an exponential decay with an increased pump pulse repetition interval. This decrease in amplitude is attributed to the characteristic decay of the acoustic wave: for lower repetition rates, the pump pulses are spaced further apart, allowing the acoustic wave to decay more, reducing the amplitude of the first copy. The amplitude of the read-out/delayed pulses shows the typical decay observed in Brillouin-based memory experiments.¹⁸

In the case of QLS, however, successive pump pulses not only create an optical copy of the original optical signal pulse but also transfer energy to the acoustic wave. Depending on the repetition rate, the acoustic wave can either lose more energy in the decay time than it receives from the pump pulse or gain more energy than it loses. In the cases of 100, 125, and 150 MHz repetition rates, the

amplitude of the copies will decay. With higher repetition rates of 175 and 200 MHz, the amplitude of the copies will increase. Our experimental study illustrates the importance of the repetition rate for QLS, which on the one hand needs to be low enough to have a fine enough comb line spacing to fulfill the Nyquist sampling theorem of the optical data but cannot be lower than the decay rate of the acoustic wave of 30 MHz. We note that tens to hundreds of MHz is quite fine for signals with multi-GHz bandwidth that are desired for many applications.

For the latter two repetition rates, 175 and 200 MHz, the growth of the copies eventually stops and then reverses; we attribute this behavior to the strong pump pulses shifting the stored acoustic wave to the front facet of the waveguide, where it is trapped and eventually decays. We note that this shift of the acoustic wave to the front facet

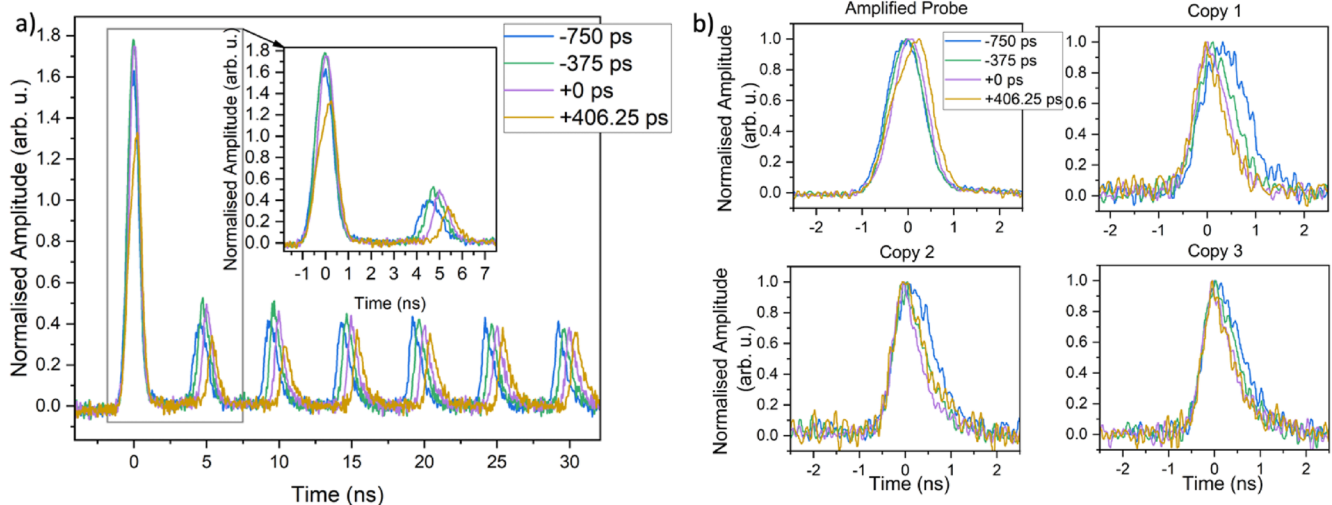


FIG. 4. Pulse timing measurements. (a) Full trace of signals with different timings relative to the middle of the chip (0 ps). The chip extends from -1000 ps on the probe side to $+1000$ ps on the pump side. The height is normalized to the amplitude of the unamplified probe. (b) The amplified probe and the first three copies, normalized to unit height and shifted in time to allow a shape comparison.

is not due to the propagation of the acoustic wave with the speed of sound through the waveguide, which would take tens of μs based on the length of the waveguide of 23 cm and an estimated speed of sound of around 2500 m/s. We investigate the behavior of the optical pulling of the acoustic wave to the front facet numerically in Sec. IV.

B. Pulse timing

We further investigate the underlying behavior of the stored acoustic wave by changing the spatial overlap of the pump pulses and the signal pulse in the waveguide. Since the transit time of the chip is ~ 2 ns, precise timing between the signal and the first pump pulse is critical to ensure that the pulses overlap in the chip. The experiments in Sec. III A were performed for the case of the pulses meeting at a point equidistant from the front and rear facets of the waveguide. This spatial overlap point can be controlled by changing the time of arrival of the individual pulses. Figure 4 shows measurements for different arrival times of the pump and signal pulses, such that the spatial pulse overlap is adjusted from the center of the waveguide (denoted as $t = 0$ ps): we show [Fig. 4(a)] delay times of -750 , -375 , and $+475$ ps, where positive (negative) delays indicate that the pulses meet closer to the front (rear) facet. In each of these measurements, we used a pump pulse train of 21 Gaussian pulses with 500 ps FWHM, a repetition rate of 200 MHz, and a peak power of 7.7 W. The probe was a 1 ns FWHM Gaussian pulse with a peak power of 19.7 W. The measurements in Fig. 4(a) show that the copied pulses that are generated from overlap points further away from the pump side, i.e., the front facet, appear earlier with each copy. This is an indication that the acoustic wave is being shifted with each pulse toward the front facet. Zoom-ins on the initial pulse and the generated copies are shown in Fig. 4(b) and reveal that the pulse shape is maintained slightly better for the case where the acoustic wave is generated further away from the front facet (note that those effects are subtle due to the similar length of the optical pulses and the waveguide transit time).

C. Shape retention

To study the effect of on-chip QLS on the retrieved pulse shape, we repeated the experiment with longer, more square-shaped (in particular, super-Gaussian) signal pulses. Figure 5 shows the storage of a 1.5 ns super-Gaussian signal pulse with a peak power of 7.8 W. The pump pulse train consisted of 500 ps Gaussian pulses with a repetition rate of 201 MHz and a peak power of 33.1 W. It can be seen that the original signal is amplified, and the pulse shape is maintained. The first copy maintains a square-like shape, although with some distortions. Subsequent copies change the shape to a more triangular form [see Fig. 5(b)] with each iteration. We attribute this to a combination of effects: first, each interaction convolves the existing acoustic field in the waveguide with the (Gaussian) pump pulse. Ideally, the pump pulses are much shorter than the signal pulse; however, that comes at the expense of Brillouin gain. Second, the acoustic wave itself is shifted to the front facet, where it is trapped and becomes progressively more exponential. We investigate this behavior in Sec. IV.

D. Ultra-long optical storage

We next studied the achievable storage times of on-chip QLS. It was observed that by adjusting pump power and repetition rates, the retrieved pulse train can enter a steady state that does not decay with time. We show such a state in Fig. 6: this response was achieved using a Gaussian signal pulse of 4.1 W with a duration of 1 ns. The pump train consisted of 101 Gaussian pump pulses with a peak pulse power of 1.8 W, a pulse duration of 1 ns, and a repetition rate of 201 MHz. For this combination, we observe storage times of about 0.5 μs (although with the same distortions in the pulse shape as described in Fig. 5 and which are further analyzed numerically in Sec. IV). This demonstrates that the acoustic wave is being restored by the action of the pump pulses; the pump pulse train cuts-off after 0.5 μs due to limitations in the experimental setup (AWG memory depth and available pump power from the EDFAs). These experiments suggest

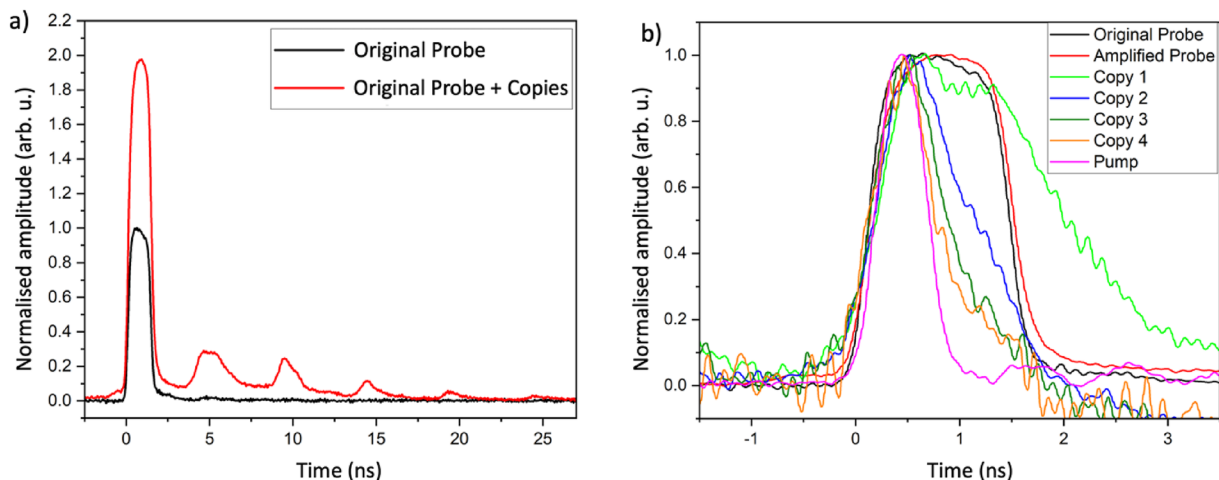


FIG. 5. Shape retention measurements of a 1.5 ns square pulse. (a) The full amplified probe and copies in time (red trace) and the original probe without the pump (black trace). (b) A zoomed-in view of all the copies normalized to the height of one laid on top of each other to show the evolution of the pulse shape with each copy. The pump pulse (pink trace) before the chip is shown and lined up as a comparison.

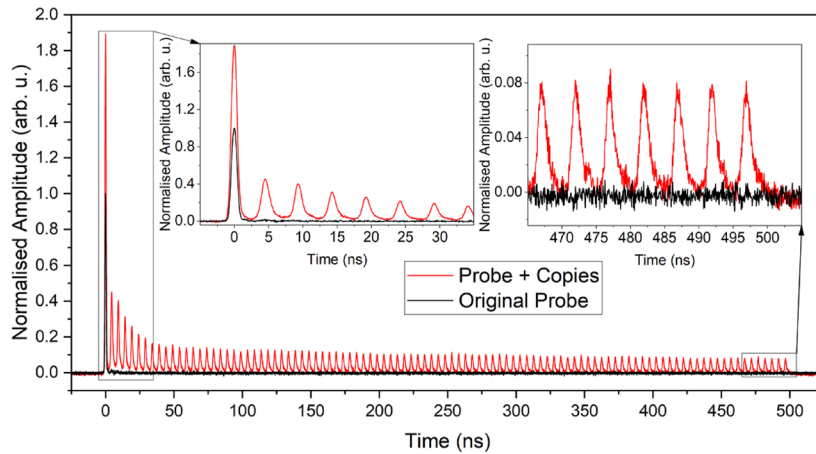


FIG. 6. Experimental results of QLS in a photonic chip reaching storage times of 500 ns of a 1 ns probe pulse (black trace). The amplitude is normalized so that the original probe pulse height is one. Black is the original probe pulse going through the chip without any SBS interaction. Red is the amplified probe, and delayed copies are caused by the SBS interaction between the pump and probe.

that storage times approaching the microsecond regime should be possible. The steady state is attributed to the pump pulse contributing energy to the acoustic wave at exactly the rate required to balance the acoustic losses. We investigate this numerically in the following section.

IV. TIME DOMAIN SIMULATIONS

To understand the experimental results and identify different regimes of QLS, we perform time-domain numerical simulations

of the storage process. The appropriate framework for describing Brillouin interactions is the coupled mode theory,²¹ in which the interaction is modeled by the following equations:

$$\left(\frac{\partial}{\partial z} + \frac{1}{v} \frac{\partial}{\partial t} + \alpha\right)a_p(z, t) = -i\omega_p Q^* a_s b, \quad (1)$$

$$\left(\frac{\partial}{\partial z} - \frac{1}{v} \frac{\partial}{\partial t} - \alpha\right)a_s(z, t) = i\omega_s Q a_p b^*, \quad (2)$$

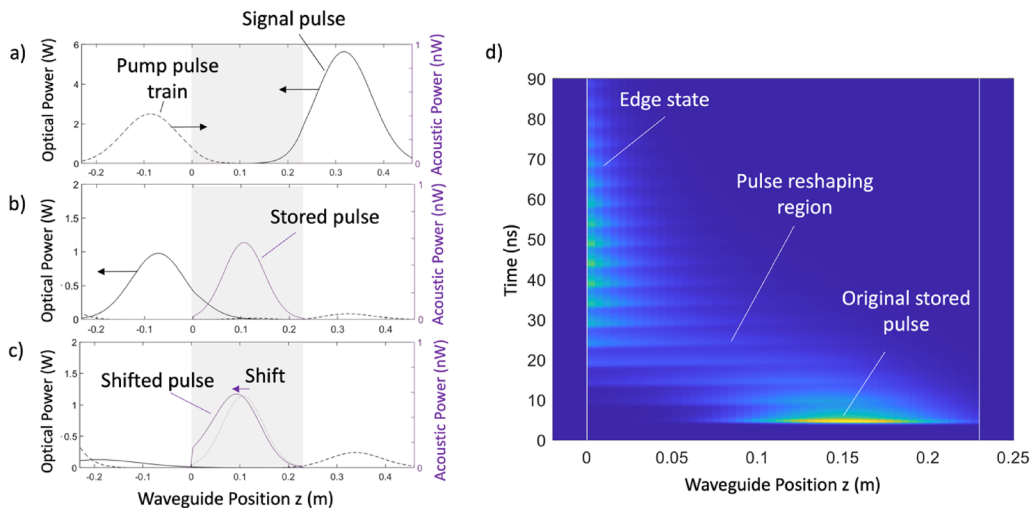


FIG. 7. (a)–(c) Computation showing the acoustic storage and pulse-reshaping process. The pump and signal pulses intersect in the waveguide [indicated in gray in the figure panels (a)–(c) and by the white lines in panel (d)]. (a) Creating a stored acoustic pulse (b). A subsequent pump pulse shifts the stored pulse toward the front facet (c). (d) Computed power in the acoustic field when the initial intersection between pump and signal pulses is 3/4 along the length of the waveguide. Repeated pump pulses refresh and reshape the stored acoustic pulse, moving the peak to the front facet of the waveguide.

05 December 2024 16:24:32

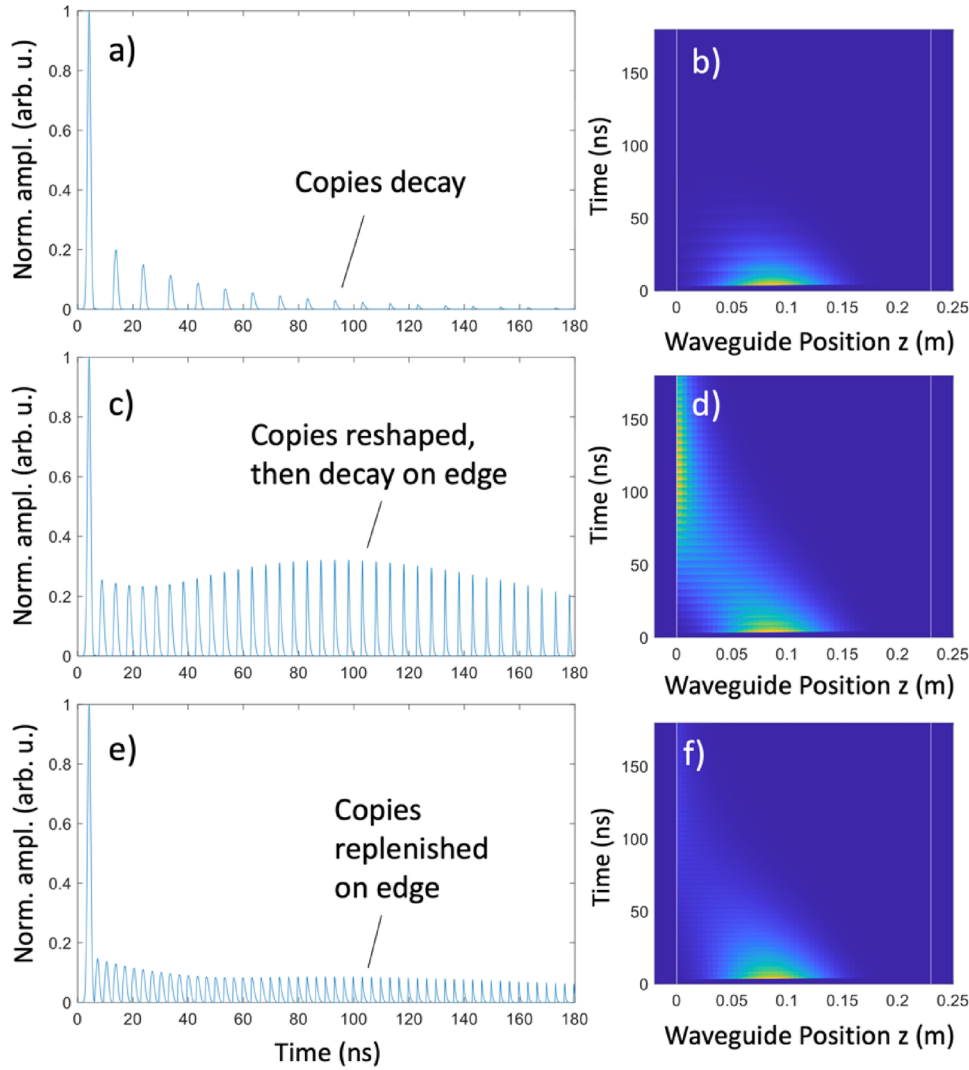


FIG. 8. Simulation of different QLS regimes. (a) Output of the retrieved signal pulse in the decaying regime, for a peak pump power of 5.0 W, a pump duration of 0.25 ns, and a repetition rate of 100 MHz. Here, the stored acoustic pulse remains within the waveguide (b) and loses energy due to acoustic losses faster than the pump wave can replenish it. (c) Retrieved signal in the reshaping regime for a peak pump power of 5.0 W, a pump duration of 0.25 ns, and a repetition rate of 200 MHz. Here, the acoustic field is shifted to the front facet of the waveguide (d), where it slowly decays. (e) Retrieved signal in the replenishing regime for pump power of 10.0 W, pump duration of 0.125 ns, and repetition rate of 300 MHz. Here, the acoustic wave is shifted to the front facet (f), where it is continuously replenished by the pump.

$$\left(\frac{\partial}{\partial z} + \frac{1}{v_{ac}} \frac{\partial}{\partial t} + \alpha_{ac} \right) b(z, t) = -i\Omega Q a_p a_s^*, \quad (3)$$

where $a_p(z, t)$, $a_s(z, t)$, and $b(z, t)$ are the amplitude of the pump, signal, and acoustic waves, respectively; $v = n/c$ and v_{ac} are the optical and acoustic modal group velocities; and α and α_{ac} are the optical and acoustic modal loss in units of m^{-1} . The frequencies of the pump, signal, and acoustic waves are ω_p , ω_s , and $\Omega = \omega_p - \omega_s$, respectively. The constant Q is a measure of the strength of the Brillouin coupling and can be computed from the overlap integrals of

the optical and acoustic mode fields.²¹ It is related to the Brillouin gain g_0 in units of $m^{-1} W^{-1}$ by $g_0 = 2\Omega\omega_s |Q|^2 / \alpha_{ac}$. Here, we have normalized each field so that the squared amplitude of the field is equal to the power carried in the mode. In the following, unless otherwise specified, we use $g_0 = 344 m^{-1} W^{-1}$, $n = 2.2$, and α is specified by the optical loss of $0.4 dB cm^{-1}$, and $\alpha_{ac} = 1/(2v_{ac}\tau_{ac})$ is given via the acoustic lifetime of $\tau_{ac} = 10 ns$. The acoustic velocity is $v_{ac} = 2500 ms^{-1}$, resulting in a Brillouin shift of $\Omega/2\pi = 7.1 GHz$.

To solve Eqs. (1)–(3), we transform each equation to appropriate co-moving coordinates and integrate the system in the time coordinate using Runge–Kutta integration.³³ We assume Gaussian

input pulses for both pump and signal waves and a zero initial acoustic field. The interaction is set to zero outside the simulated waveguide domain, $0 \leq z \leq L$.

In Fig. 7, we show the time-dependent solution to Eqs. (1)–(3) for a stored optical pulse. In Fig. 7(a), the initial signal and pump pulses intersect in the center of the waveguide, creating an acoustic field. A subsequent pump pulse interacts with the acoustic field, losing energy in the process and generating an output Stokes wave [Fig. 7(b)]. Because the interaction between the pump and the acoustic wave scales linearly with the amplitude of the Stokes field, the acoustic wave is amplified more strongly on the left (output) side of the pulse. This leads to an overall shift in the acoustic field toward the front facet of the waveguide [Fig. 7(c)]. It should be noted that this shift is many orders of magnitude larger than the shift caused by the propagation of the acoustic wave, which will travel a distance of $12.5 \mu\text{m}$ in the 5 ns between optical pulses. Once reaching the front facet, the acoustic wave cannot be shifted further and only propagates extremely slowly away from the facet. The acoustic excitation will therefore remain in the vicinity of the facet, steadily decaying until the arrival of the next pump pulse. Repeated pump pulses continue this reshaping process until the acoustic field strikes the front facet of the waveguide [Fig. 7(d)].

The strength and repetition rate of the pump can lead to different regimes for QLS in finite waveguides. We show representative simulations of these regimes in Fig. 8. For low repetition rates/weak pumps [Figs. 8(a) and 8(b)], the acoustic field decays faster than the pump can replenish it; in this case, the copies of the original signal pulse decay exponentially. At higher pump repetition rates [Figs. 8(c) and 8(d)], the acoustic field is reshaped and pushed toward the front facet of the waveguide, where it is continually replenished. At this point, the copies of the signal will either slowly decay (if the pump is weak) or be amplified (if the pump is sufficiently strong). For particular combinations of pump strength and duration, the trapped acoustic mode will lose energy at exactly the same rate that energy is gained from the pump. This situation is

shown in Figs. 8(e) and 8(f); the output copies of the signal can be maintained for extended time periods.

In Fig. 5, it was observed that QLS can lead to significant distortion of the original probe pulse. We investigate this distortion numerically in Fig. 9, where we show the QLS of a super-Gaussian pump in the reshaping regime. For successive copies, we observe that the initial square shape is quickly lost, not only from successive convolutions with the (Gaussian) pump but also because the acoustic field, which stores the information about the pulse shape, is compressed against the waveguide edge, forming a truncated exponential. This compression in space also causes the acoustic field, as well as the output copies of the signal, to become compressed in the time domain [see Fig. 9(b)]. We also see that the leading edges of the copies arrive sooner at the output—this is because the pump interacts earlier with the acoustic field as the latter is pulled toward the front facet of the waveguide (as observed experimentally; see Fig. 6).

V. DISCUSSION

The experiments and numerical results presented here highlight a qualitative difference between quasi-light storage in a quasi-infinitely extended fiber and QLS on a chip. In the fiber case, the pump frequency comb is used to spectrally sample the data; the optical information is then stored in a series of acoustic pulses spaced along the length of the waveguide, each centered at a point where a part of the pump pulse train interacts with the data pulse. The absolute positions of the acoustic pulses within the waveguide therefore do not matter as much as their separation. The on-chip case, however, is constrained in space, allowing only a single acoustic mode to be created, at least in cm-scale waveguides. In this case, the position of the acoustic wave is critical: the pump pulse train continuously replenishes and reshapes it, moving it steadily to the waveguide front facet; if the optical loss is high, then the acoustic field may be moved

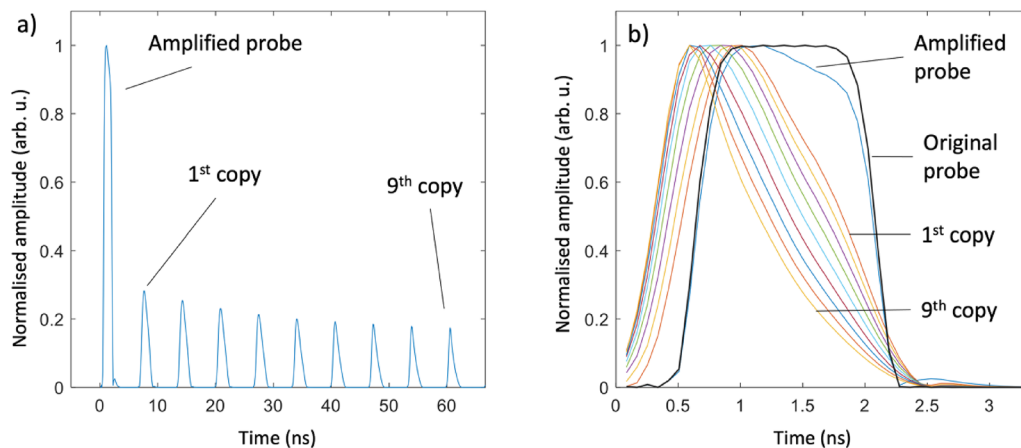


FIG. 9. (a) Output of a stored and recovered super-Gaussian probe, showing pulse distortion. Repeated copies modify the initial super-Gaussian into a triangular form with a trailing edge. The pulses are overlaid in (b) to emphasize the distortion. The leading edges of the copied pulses shift in time as the acoustic pulse is shifted toward the edge of the waveguide. The probe is a fourth-order super-Gaussian with a peak power of 1.0 W and a FWHM of 1.5 ns. The pump is a Gaussian with a peak power of 5.0 W, an FWHM of 0.25 ns, and a repetition rate of 150 MHz.

rapidly to a position where the pump is highest in amplitude, reaching the end of the waveguide and thereby reducing the strength of the interaction.

The continuous replenishment of the acoustic field, contingent on the input pump balancing the acoustic losses, enables the sustainment of the acoustic grating within the waveguide, which is much longer than anything previously shown in Brillouin storage. Because there is only one acoustic mode, the bandwidth of the optical information that can be stored is constrained, and this results in the loss of the data pulse shape, particularly when the acoustic field encounters the end of the waveguide. It is conceivable that this distortion is not an inevitable feature of on-chip QLS, and we propose several remedies to reduce it: first and foremost, shorter pump pulses can be used; these will better maintain the data pulse/acoustic wave packet shape on each pass. Such shortening of the pump must, however, be accompanied by an increase in optical peak power to balance the acoustic losses. Second, it should be possible to use longer waveguides, such that the acoustic field does not encounter the edges, or else employ an off-resonant ring waveguide. More complicated options for controlling the acoustic field include engineering the acoustic and optical waveguide dispersion to trap the acoustic mode within the center of the waveguide or the use of optical chirp to tailor distortion-resistant pulses. We leave these investigations to future work.

VI. CONCLUSION

We have demonstrated SBS-based QLS on a photonic chip, achieving single pulse delay times of hundreds of pulse widths. The optical pulses are stored in a single acoustic wave on the chip created via the strong Brillouin interaction between spatially overlapping signal and pump pulses enabled by tailor-made chalcogenide waveguides. Our insight into storing the optical information in the acoustic wave while it is copied via the QLS process allowed us to overcome the requirements for km-long optical fiber. In a steady state regime where consecutive pump pulses counteract the acoustic decay, we show one ns long optical pulses delayed for up to 500 ns, exceeding the intrinsic phonon lifetime by more than an order of magnitude and the waveguide transit time by more than two orders of magnitude. We numerically and experimentally studied the dynamics of on-chip QLS and the replenishing effect of the acoustic wave. We found a rapid pulling and reshaping effect of the acoustic wave toward the chip front facet and identified it as a source of distortion in the pulse shape. Future work will focus on mitigating the pulling effect to minimize distortions of the pulses. Our work reveals a new regime of QLS in short waveguides and opens a pathway to further integration and miniaturization for applications in Size, Weight, and Power (SWaP) constrained environments.

ACKNOWLEDGMENTS

We acknowledge the support of the Australian Research Council (Grant Nos. DP220101431 and DP200101893) and the ANFF OptoFab ACT Node in carrying out this research. This research was supported by the Australian Research Council Center of Excellence in Optical Microcombs for Breakthrough Science (Project No. CE230100006) and funded by the Australian Government. We

would also like to acknowledge Professor David Marpaung, Dr. Birgit Stiller, Professor Amol Choudhary, Dr. Stefan Preussler, and Professor Thomas Schneider for fruitful discussions.

AUTHOR DECLARATIONS

Conflict of Interest

The authors have no conflicts to disclose.

Author Contributions

M.M. and L.G. authors contributed equally to this work.

Moritz Merklein: Conceptualization (equal); Investigation (equal); Methodology (equal); Supervision (equal); Writing – original draft (equal); Writing – review & editing (equal). **Lachlan Goulden:** Data curation (equal); Formal analysis (equal); Investigation (equal); Methodology (equal); Software (equal); Validation (equal); Writing – original draft (equal); Writing – review & editing (equal). **Max Kiewiet:** Investigation (equal); Methodology (equal); Writing – review & editing (equal). **Yang Liu:** Conceptualization (equal); Investigation (equal); Methodology (equal); Writing – review & editing (equal). **Choon Kong Lai:** Investigation (equal); Methodology (equal); Writing – review & editing (equal). **Duk-Yong Choi:** Investigation (equal); Methodology (equal); Writing – review & editing (equal). **Stephen J. Madden:** Investigation (equal); Methodology (equal); Resources (equal); Writing – review & editing (equal). **Christopher G. Poulton:** Data curation (equal); Formal analysis (equal); Methodology (equal); Software (equal); Validation (equal); Visualization (equal); Writing – original draft (equal); Writing – review & editing (equal). **Benjamin J. Eggleton:** Conceptualization (equal); Investigation (equal); Project administration (equal); Resources (equal); Supervision (equal); Writing – review & editing (equal).

DATA AVAILABILITY

The data that support the findings of this study are available from the corresponding author upon reasonable request.

REFERENCES

- S. Pan, X. Ye, Y. Zhang, and F. Zhang, “Microwave photonic array radars,” *IEEE J. Microwaves* **1**, 176–190 (2021).
- M. Garrett, M. Merklein, and B. J. Eggleton, “Chip-based Brillouin processing for microwave photonic phased array antennas,” *IEEE J. Sel. Top. Quantum Electron.* **29**, 7600220 (2023).
- E. Furmeister, D. J. Blumenthal, and J. E. Bowers, “A comparison of optical buffering technologies,” *Opt. Switching Networking* **5**, 10–18 (2008).
- A. I. Lvovsky, B. C. Sanders, and W. Tittel, “Optical quantum memory,” *Nat. Photonics* **3**, 706–714 (2009).
- J. Sancho *et al.*, “Integrable microwave filter based on a photonic crystal delay line,” *Nat. Commun.* **3**, 1075 (2012).
- L. Z. Linjie Zhou, X. W. Xinyi Wang, L. L. Liangjun Lu, and J. C. Jianping Chen, “Integrated optical delay lines: A review and perspective [Invited],” *Chin. Opt. Lett.* **16**, 101301 (2018).
- S. Chin and L. Thévenaz, “Tunable photonic delay lines in optical fibers,” *Laser Photonics Rev.* **6**, 724–738 (2012).

- ⁸K. Y. Song, K. Lee, and S. B. Lee, “Tunable optical delays based on Brillouin dynamic grating in optical fibers,” *Opt. Express* **17**, 10344–10349 (2009).
- ⁹H. Park, J. P. Mack, D. J. Blumenthal, and J. E. Bowers, “An integrated recirculating optical buffer,” *Opt. Express* **16**, 11124–11131 (2008).
- ¹⁰T. Baba, “Slow light in photonic crystals,” *Nat. Photonics* **2**, 465–473 (2008).
- ¹¹T. F. Krauss, “Slow light in photonic crystal waveguides,” *J. Phys. D: Appl. Phys.* **40**, 2666–2670 (2007).
- ¹²L. V. Hau, S. E. Harris, Z. Dutton, and C. H. Behroozi, “Light speed reduction to 17 metres per second in an ultracold atomic gas,” *Nature* **397**, 594–598 (1999).
- ¹³J. T. Mok, C. M. de Sterke, I. C. M. Littler, and B. J. Eggleton, “Dispersionless slow light using gap solitons,” *Nat. Phys.* **2**, 775–780 (2006).
- ¹⁴S. Weis *et al.*, “Optomechanically induced transparency,” *Science* **330**, 1520–1523 (2010).
- ¹⁵Y. Okawachi *et al.*, “Tunable all-optical delays via Brillouin slow light in an optical fiber,” *Phys. Rev. Lett.* **94**, 153902 (2005).
- ¹⁶K. Y. Song, M. Herráez, and L. Thévenaz, “Observation of pulse delaying and advancement in optical fibers using stimulated Brillouin scattering,” *Opt. Express* **13**, 82–88 (2005).
- ¹⁷Z. Zhu, D. J. Gauthier, and R. W. Boyd, “Stored light in an optical fiber via stimulated Brillouin scattering,” *Science* **318**, 1748–1750 (2007).
- ¹⁸M. Merklein, B. Stiller, K. Vu, S. J. Madden, and B. J. Eggleton, “A chip-integrated coherent photonic-phononic memory,” *Nat. Commun.* **8**, 574 (2017).
- ¹⁹R. W. Boyd, *Nonlinear Optics* (Academic Press, 2008).
- ²⁰M. Merklein, I. V. Kabakova, A. Zarifi, and B. J. Eggleton, “100 years of Brillouin scattering: Historical and future perspectives,” *Appl. Phys. Rev.* **9**, 041306 (2022).
- ²¹C. Wolff, M. J. Steel, B. J. Eggleton, and C. G. Poulton, “Stimulated Brillouin scattering in integrated photonic waveguides: Forces, scattering mechanisms, and coupled-mode analysis,” *Phys. Rev. A* **92**, 013836 (2015).
- ²²M. Merklein, B. Stiller, and B. J. Eggleton, “Brillouin-based light storage and delay techniques,” *J. Opt.* **20**, 083003 (2018).
- ²³Z. Zhu *et al.*, “Numerical study of all-optical slow-light delays via stimulated Brillouin scattering in an optical fiber,” *J. Opt. Soc. Am. B* **22**, 2378 (2005).
- ²⁴B. J. Eggleton, C. G. Poulton, P. T. Rakich, M. J. Steel, and G. Bahl, “Brillouin integrated photonics,” *Nat. Photonics* **13**, 664 (2019).
- ²⁵R. Pant *et al.*, “Photonic-chip-based tunable slow and fast light via stimulated Brillouin scattering,” *Opt. Lett.* **37**, 969 (2012).
- ²⁶J. B. Khurgin, “Optical buffers based on slow light in electromagnetically induced transparent media and coupled resonator structures: Comparative analysis,” *J. Opt. Soc. Am. B* **22**, 1062 (2005).
- ²⁷B. Stiller *et al.*, “Coherently refreshing hypersonic phonons for light storage,” *Optica* **7**, 492 (2020).
- ²⁸S. Preußler *et al.*, “Quasi-light-storage based on time-frequency coherence,” *Opt. Express* **17**, 15790–15798 (2009).
- ²⁹K. Jamshidi, S. Preussler, A. Wiatrek, and T. Schneider, “A review to the all-optical quasi-light storage,” *IEEE J. Sel. Top. Quantum Electron.* **18**, 884–890 (2012).
- ³⁰S. Preussler, A. Wiatrek, K. Jamshidi, and T. Schneider, “Quasi-light-storage enhancement by reducing the Brillouin gain bandwidth,” *Appl. Opt.* **50**, 4252–4256 (2011).
- ³¹C. K. Lai *et al.*, “Hybrid chalcogenide-germanosilicate waveguides for high performance stimulated Brillouin scattering applications,” *Adv. Funct. Mater.* **32**, 2105230 (2022).
- ³²C. G. Poulton, R. Pant, and B. J. Eggleton, “Acoustic confinement and stimulated Brillouin scattering in integrated optical waveguides,” *J. Opt. Soc. Am. B* **30**, 2657–2664 (2013).
- ³³O. A. Nieves, M. D. Arnold, M. J. Steel, M. K. Schmidt, and C. G. Poulton, “Noise and pulse dynamics in backward stimulated Brillouin scattering,” *Opt. Express* **29**, 3132 (2021).